Impact of drying and carbonation on microstructure and dimensional changes for supplementary cementitious materials (SCMs)

BERTIN Matthieu[1, a *], OMIKRINE METALSSI Othman[1,b], BAROGHEL BOUNY Véronique[1,c] and OURO KOURA Baba Issa[1]

[1] Université Paris-Est, MAST, FM2D, IFSTTAR, F-77447 Marne-la-Vallée, France

[a]matthieu.bertin@ifsttar.fr, [b]othman.omkrine-metalssi@ifsttar.fr, [c]veronique.baroghel-bouny@ifsttar.fr

*corresponding author

Keywords: Shrinkage, microstructure, slag, carbonation, drying.

Abstract.

Carbonation is one of the main causes of reinforced concrete damage. It leads to decrease the pH of the concrete pore solution which leads to the depassivation and the corrosion of rebar. The mechanisms of carbonation are complex in low-clinker cementitious materials. The consequences are microstructure changes leading to the dimensional variations and consequently to the crack appearance. The low-clinker cementitious materials named also supplementary cementitious materials (SCMs) can become less resistant against this phenomenon. In this case, the impact of carbonation on microstructure and shrinkage can be more significant than for ordinary cement materials. The results of this work confirm that the carbonation resistance is lower for the ground granulated blastfurnace slag GGBS than CEM I cement paste which is in agreement with the finding that the drying and carbonation shrinkages are higher for this SCMs than the CEM I mortars. In the case of ordinary cement paste (CEM I), the carbonation of Portlandite and high quantities of aluminates and C-S-H produces a higher content of $CaCO_3$. .

Introduction

Corrosion is one of the more hazardous damage process affecting the reinforced concrete and leading to the stiffness, strength decrease and finally the general structural damage [1]. The two main depassivation mechanisms of steel reinforcement in concrete are chloride attack [2], [3] and carbonation [4]. This last phenomenon is the consequence of the interaction between the hydrates (Portlandite, C-S-H and Aluminates) and the CO_2 leading to the formation of $CaCO_3$ and water [Cf. Equations 1 & 2]. The consequences of this reaction are a decrease of porous solution pH with the consumption of Portlandite, microstructure change due to the dissolution of hydrate and the precipitation of $CaCO_3$ allowing the decrease of the porosity for both CEM I and SCMs [5], [6]. However, the SCMs remains more sensitive to the carbonation with their lower Portlandite content [7], [8].

$$CO_{2(g)} + Ca(OH)_2 \rightarrow CaCO_3 + H_2O \quad (1)$$

$$C_xSH_z + xCO_{2(g)} \leftrightarrow xCaCO_3 + SH_t + (z-t)H_2O \quad (2)$$

The changes in the microstructure lead to an increase of shrinkage [9]–[12]. The Carbonation shrinkage can be explained by several mechanisms. The first one is an additional drying shrinkage due to the production of water during the carbonation as shown by equations 1 & 2. The second mechanism link the carbonation shrinkage to C-S-H carbonation. Indeed, this reaction leads to the polycondensation of C-S-H caused by the condensation of Si-OH to yield siloxane bonds. Then, a spontaneous contraction takes place like a syneresis [13]. Furthermore, most literature and laboratory investigations on the carbonation shrinkage are based on mortar or concrete with ordinary

cement, and few works were focused on the SCMs. The use of this last type of materials causes a decrease in the $Ca(OH)_2$ content due to the dilution of clinker and its consumption by the pozzolanic reaction. In the blended cements, the carbonation resistance is lower than the ordinary cement (CEM I), as the Portlandite content decreases and the C-S-H content increases. Therefore, this suggest an increase of the carbonation shrinkage when SCMs are used.

In this paper, the effects of the coupling between carbonation and drying on pore structure, the microstructure and saturation profiles are studied on cement paste for both cement pastes (CEM I and SCMs). Shrinkage is studied on mortar because this material is more realistic than cement paste. The results of this mechanism are presented and discussed.

Materials and methods

Materials and conservation

Two paste systems (CEM I (PCM) and CEM I with replacement by 60% GGBS (Ground Granulated Blastfurnace Slag) (P6S), representing the SCMs used in this study, with W/B ratio of 0.57 were investigated. The replacement in the manufacture of the two systems was by volume. The chemical composition of CEM I 52.5 R and SMCs were determined by X-ray fluorescence (XRF) [Table 1]. The clinker phase contents are calculated according to Bogue's approach and shown in Table 2. The Blaine fineness is 4740 cm^2/g for the GGBS and 4900 cm^2/g for the CEM I.

Table 1: Chemical composition of raw materials

	LOI	SiO_2	Al_2O_3	Fe_2O_3	TiO_2	MnO	CaO	MgO	SO_3	K_2O	Na_2O	P_2O_5
CEM I 52.5R (%)	1.50	20.50	4.60	2.40	0.30	0,00	63.40	2.00	3.60	0.74	0.13	0.30
GGBS (%)	(+1.33)	36.06	11.22	0.38	0.74	0.22	41.75	6.20	2.84	0.52	0.19	0.01

Table 2: Mineralogical composition of CEM I 52.5R

	C_3S	C_2S	C_3A	C_4AF
CEM I 52,5R (%/cement)	68	10	9	7

Cement paste specimens were cast in PVC moulds (Ø=5.5 cm, h=19 cm) and were unmoulded after 24h. Then, they were kept in water during 48h. After this curing time (t_0=3 days), some samples were sawn. 3 cm of each sample on the top and the bottom were removed to limit the heterogeneity. Two kinds of samples were produced: cut and uncut [Fig. 1]. The uncut samples were used to validate results of the cut samples by comparison between the mass loss kinetics of the two kinds of samples. The samples cut in slices allow obtaining the porosity and the saturation profiles.

After this sawing operation, the bottom and the lateral sides of each specimen were sealed with two layers of aluminium foil sheets to ensure an unidirectional moisture transfer in the samples. All samples were kept in a chamber with a relative humidity (RH) of 65% at T=20°C in an environment without CO_2 (use of soda lime to trap CO_2 in the chamber). After t_0+28 days, a part of samples were put in an environment with T=20°C, RH=65% and [CO_2]=3% in an accelerated carbonation chamber. Throughout the rest of the article, the only drying condition is named condition "D" and the coupled drying-carbonation condition is named condition "C". Characterisations using different techniques presented thereafter were performed on the samples at t_0=3 days, t_0+7, t_0+28, t_0+56 and t_0+118 days. In addition to these characterisations, weight monitoring was carried out for all samples.

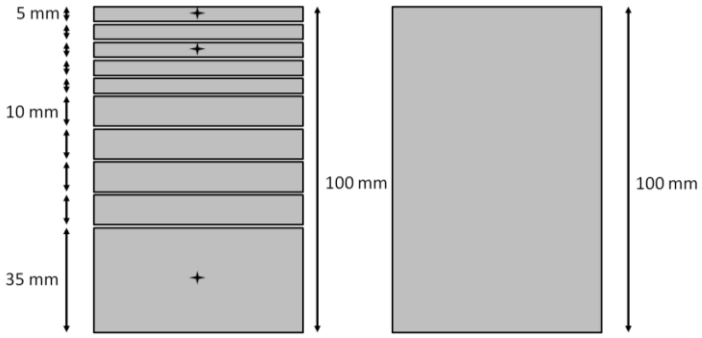

Figure 1: Cut and uncut samples used in this study (MIP and TGA measurements are carried out on slices with +)

On the other hand, two mortars (MCM and M6S) according to the proportions given in Table 3 were investigated for shrinkage because this part of the study can't be performed on cement paste (not realistic material). The cement type is the same ordinary Portland cement (OPC) CEM I 52.5R used in the first part of this study and the sand is a standard one. The other mortar is composed of CEM I and 60% of GGBS.

Table 3 : Mix proportions

	Sand [kg/m^3]	CEM I 52.5R [kg/m^3]	GGBS [kg/m^3]	water [kg/m^3]	Water/Binder	C_s at 28 days [MPa]
MCM	1333.6	444.5	-	355.6	0.80	21.2
M6S	1333.6	177.8	249.8	355.6	0.83	21.7

Prismatic samples (40x40×160 mm) [Fig. 2] were manufactured and demoulded 24h after casting. After 28 days of curing under water, the specimens were sealed on their lateral faces by aluminium foil sheets in order to impose the drying only in the longitudinal direction and to ensure unidirectional CO_2 diffusion during accelerated carbonation test. Then, specimens were dried using an oven at 45 ° C and a relative humidity (RH) of 65% for 28 days. After that, the samples were divided into two parts: the first one was exposed at a temperature of 20 ° C, RH = 65 % and [CO_2] = 0% (trap with soda lime) which corresponds to the case of drying. The second part used mainly to study carbonation was exposed to the same conditions of temperature and relative humidity but with [CO_2] = 10% in an incubator.

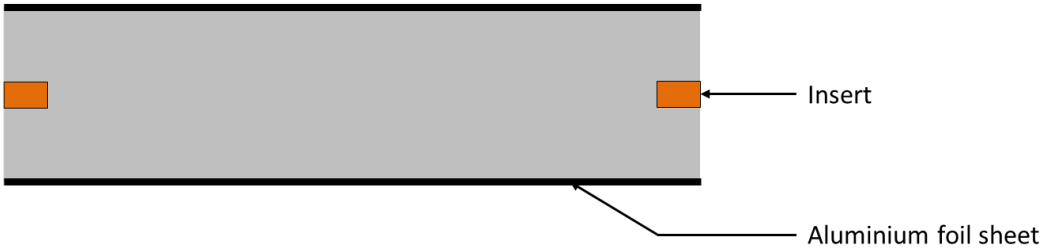

Figure 2: Specimen description

Methods

Accelerated carbonation test was carried out at T=20°C, RH=65%, [CO_2]=3% for cement paste and [CO_2]=10% for mortar.

The carbonation depths were measured at different time using a coloured indicator (phenolphthalein) sprayed on the sections of the split samples. This indicator allows distinguishing the pH ranges by separating between values above or below 9. The non-colored zone (pH<9) is considered totally carbonated while the purple zone (pH > 9) is not fully carbonated.

Saturation degree was obtained by hydrostatic weighting and drying at 80°C. This measurement is performed on 3 samples. For Thermogravimetric analysis (TGA) and Mercury Intrusion

Porosimetry (MIP) analyses, samples were freeze dried for 72h at P=0.1 mbar. These measurements are performed on one sample at each measurement time. TGA was performed in a NETZSCH STA 409E instrument under nitrogen atmosphere for samples with GGBS and under air for the other samples, heating from 25°C to 1250°C with a heating speed of 10°C/min. For the samples with GGBS substitution, a nitrogen atmosphere is used to prevent slag compounds oxidation which leads to an increase of sample mass. This technique was used to quantify the amount of $Ca(OH)_2$ and $CaCO_3$. The mass losses are measured by the derivative method because this method is appeared to be reproducible in addition to the ease of its application. The Portlandite content is calculated from Eq. 3 and the $CaCO_3$ content from Eq. 4.

$$x_{CH} = \frac{\Delta m_{T_1 \to T_2}}{m_{s\_T=1100°C}} \cdot \frac{MW_{CH}}{MW_w} \cdot 100 \quad (3)$$

where x_{CH} (%) is the Portlandite content per g of cement, $\Delta m_{T_1 \to T_2}$ (g) is the mass loss between T_1=465°C and T_2=560°C in the CEM I case and between T_1=430°C and T_2=530°C for the GGBS case, $m_{s\_T=1100°C}$ (g) is the sample mass at T=1100°C, MW_{CH} (g.mol^{-1}) is the Portlandite molecular weight and MW_w (g.mol^{-1}) is the water molecular weight.

$$x_{C\bar{C}} = \frac{\Delta m_{T=560°C \to T=1100°C}}{m_{s\_T=1100°C}} \cdot \frac{MW_{C\bar{C}}}{MW_{CO_2}} \cdot 100 \quad (4)$$

where $x_{C\bar{C}}$ (%) is the calcium carbonate content per g of cement in percent, $\Delta m_{T=560°C \to T=1100°C}$ (g) mass loss between T=560°C and T=1100°C, $m_{s\_T=1100°C}$ (g) sample mass at T=1100°C, $MW_{C\bar{C}}$ (g.mol^{-1}) calcium carbonate molecular weight and MW_{CO_2} (g.mol^{-1}) CO_2 molecular weight.

Furthermore, pore size distribution was obtained by MIP with a commercial porosimeter (Micromeritics' *AutoPore IV* 9500 Series) using a maximum intrusion pressure of 400 MPa. This technique is used to assess the pore size distribution in a comparable manner and to obtain a qualitative evolution of this pore size distribution. The porosity obtained by MIP is calculated as the mercury intrusion volume.

Finally, dimensional variation tests were carried out in accordance with the French standard procedure NF P15-433 using a retractometer. The measurement started just after water-curing. The length difference between specimen and a reference invar rod of 160 mm long is read thanks to insert fixed on the specimens during casting [Fig. 2]. The value of shrinkage ε (µm/m) is obtained.

Results and discussion

Mass loss and carbonation kinetics

Evolution of mass loss per drying surface versus the square root of time is shown in Fig. 3a for the CEM I cement paste and CEM I +60% GGBS. In the CEM I paste case, the evolution is linear. Therefore, there is no significant change in the microstructure during drying within the investigated period. In the CEM I +60% GGBSSCMs pastes case, the evolution is not linear versus square root time. The slope change takes place around one week. This change is due to a significant modification in the microstructure which leads to a lower apparent diffusivity when the GGBS reactions take place. Before one week, P6S (-1000 g.m^{-2}.d$^{-0.5}$) dries faster than PCM (-420 g.m^{-2}.d$^{-0.5}$), whereas after one week P6S (-120 g.m^{-2}.d$^{-0.5}$) dries slower.

The results of carbonation kinetics obtained by the measurement of carbonation depth with phenolphthalein spray test are shown in Fig. 3b. At 28 carbonation days for both binders, the carbonation depths are similar. One possible explanation is that, at early age, drying is slower than the carbonation. This explanation need to be confirmed. However, at 91 carbonation days, the carbonation depth for CEM I+60% GGBS is higher (5.4 mm) than CEM I (2.3 mm). The pH of CEM I +60% GGBS paste pore solution and the Portlandite content are lower than for CEM I paste.

Therefore the pH of CEM I +60% GGBS is reduced faster below the colour change of the phenolphthalein indicator.

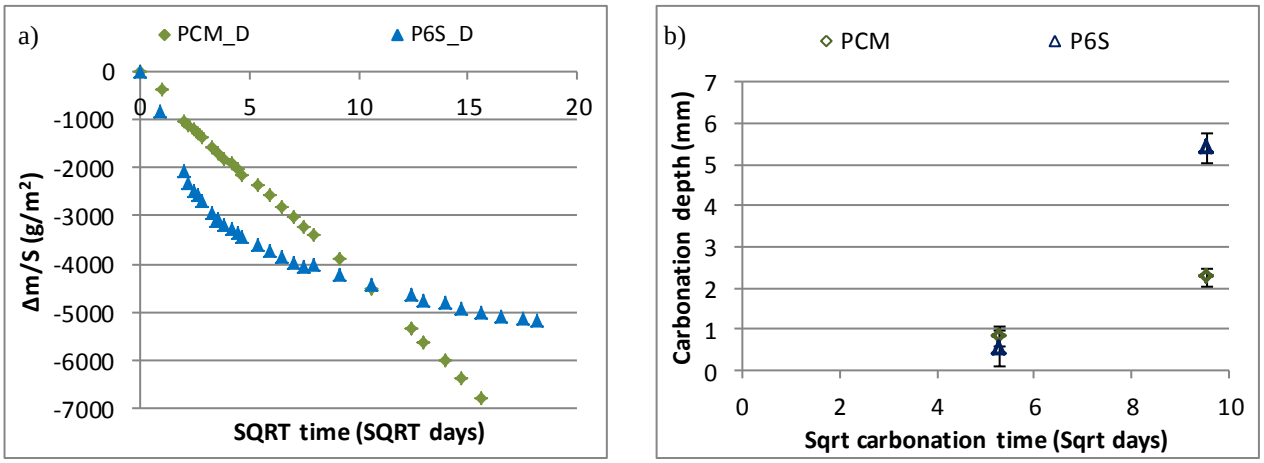

Figure 3: Evolution of mass variation to drying surface ratio (a) and carbonation depth (b) versus the square root of time for PCM and P6S

Microstructure

Fig. 4a shows the evolution of Portlandite content with time and depth for CEM I cement paste. At t_0, the Portlandite content per g of cement is the same in the entire sample and around 24%. For each depth, the Portlandite content increases with the time between t_0 and 28 days. This is due to the hydration of clinker. Moreover, in the condition D, the Portlandite content is constant for a time longer than 28 days. This finding is the same in the condition D where the Portlandite content is also the same at the depths of 1-1.5 cm. the Portlandite content is constant for a time longer than 56 days at the depth of 6.5-10.0 cm. This Portlandite content in the GGBS cementSCMs paste [Fig. 4b] is lower than in the CEM I cement paste. This is due to the clinker dilution. The same trends are observed for P6S than PCM. Nevertheless, at the depth of 0-0.5 cm, the Portlandite contents decrease due to carbonation which is confirmed by the Fig. 5 a & b where the $CaCO_3$ contents are constant at all the time except for the surface in the condition C for both binders. In the Table 4, for both binders the ratio is above 1, therefore C-S-H and Aluminates are carbonated. The carbonation of C-S-H is higher for the P6S (ratio = 6 at a carbonation time =90 days) than PCM (ratio = 1.8 at a carbonation time=90 days). For both binders, at all the time in the condition D, the $CaCO_3$ contents near to the surface are higher than the other depths. This is due to the carbonation of a thin layer at the surface.

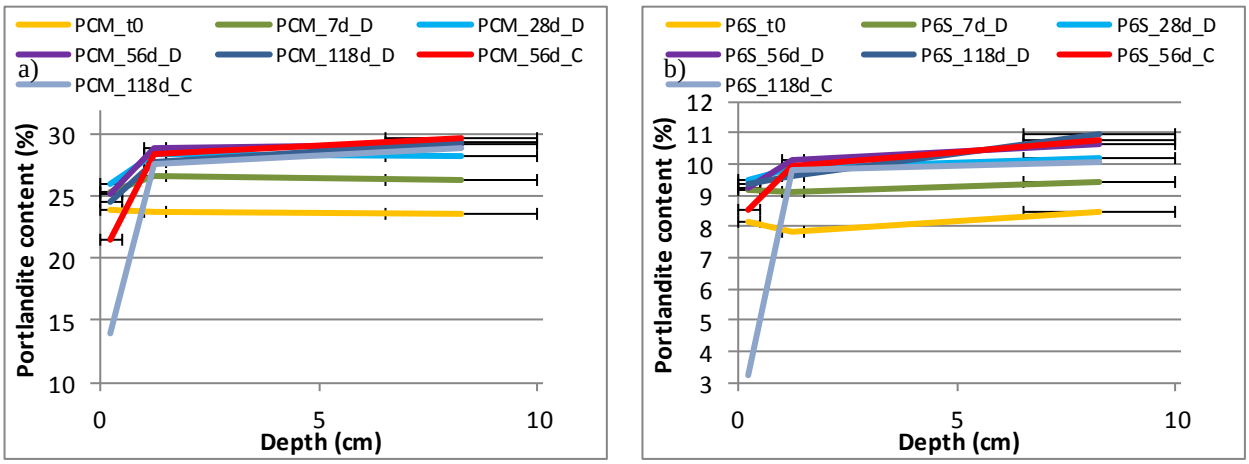

Figure 4: Evolution of Portlandite content with time for PCM (a) and for P6S (b)
D: drying condition – C: coupled drying and carbonation conditions

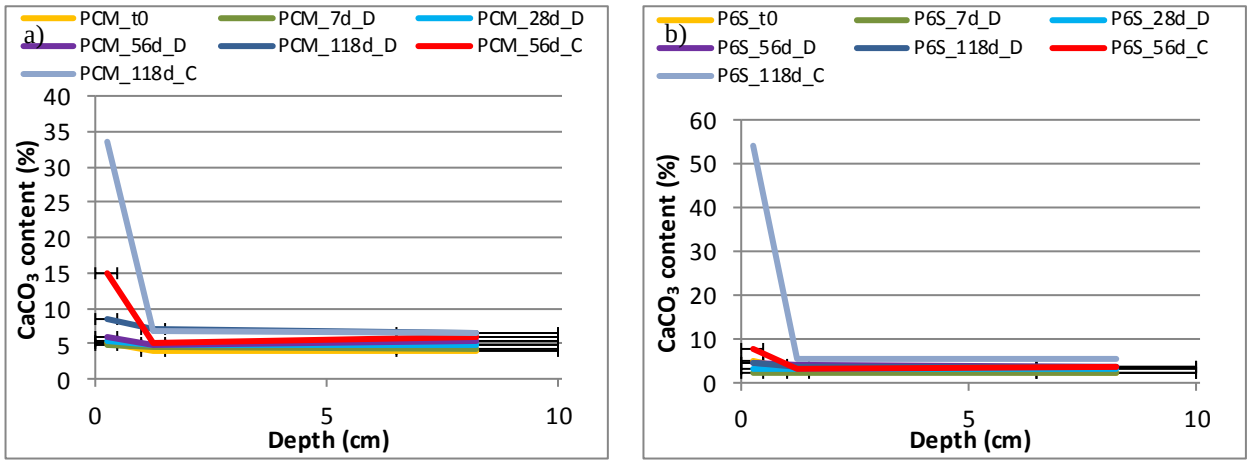

Figure 5: Evolution of $CaCO_3$ content with time for PCM (a) and for P6S (b), D: drying condition – C: coupled drying and carbonation conditions

Table 4 : molar variation of CaCO3 to molar variation of Portlandite ratio

	PCM		P6S	
Carbonation time [days]	28	90	28	90
$\Delta n_{C\bar{C}} / \Delta n_{CH}$	1.8	1.8	3.5	6.0

Pore structure

Fig.6a shows the pore size distribution at the surface for the CEM I cement paste. In the condition D, the pore structure becomes a little coarser versus the time while the porosity decreases during the hydration process. For the slag cement paste [Figure 6b], the main pore diameter decreases a little and a second peak appears around 6 nm. These changes can be explained by the hydration of clinker and the GGBS reaction.

Fig. 7a shows a comparison of the pore size distribution at the surface for PCM between the conditions D and C. The main pore diameter decreases in the condition C. The porosity obtained by MIP is 34.5 % at 118 days in the condition D and 31.3 % in the condition C. This pore structure change can be explained by the filling of the porosity by the $CaCO_3$ which leads to decrease the main pore diameter. For the P6S [Figure 7b], the bigger pore does not change in both condition whereas the smaller pore diameter increases after 118 days in the condition C. Moreover, the porosity obtained at 118 days in the condition D is 40.8 % and 32.1 % in the condition C. This change can be explained by a change of pore structure of gel due to the carbonation of C-S-H which leads to a coarser porosity whereas the precipitation of $CaCO_3$. At the core of CEM I cement paste [Fig. 7a], the pore diameter decreases between t_0 and t_0+118 days from 220 nm to 20 nm due to hydration process. The same trend is observed for the blended slag paste where the pore diameter decreases from 630 nm to 6 nm. At the depth of 6.5-10.0 cm, samples are subjected to neither drying nor carbonation. At the surface, the GGBS pastes have a coarser porosity than the CEM I cement paste due to the drying which stops the hydration. The GGBS cement pastes have a finer pore structure than the CEM I cement paste one at a depth of 6.5-10.0 cm without drying.

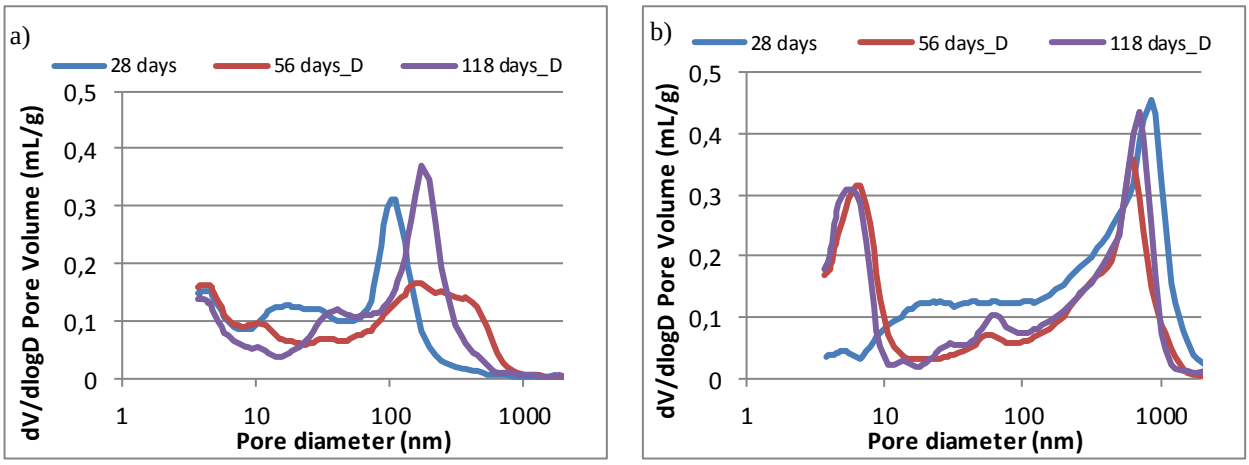

Figure 6: Evolution of the pore size distribution for PCM (a) and for P6S (b) at a depth of 0.0-0.5 cm in the drying condition (D)

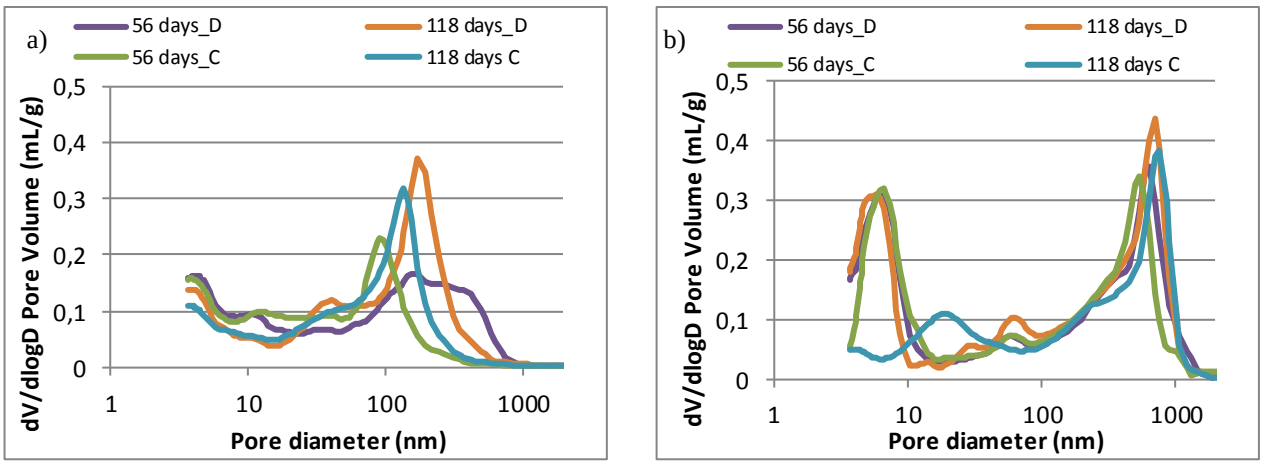

Figure 7: Comparison of the pore size distribution between the conditions D & C for the PCM (a) and for P6S (b) at a depth of 0.0-0.5 cm
D: drying condition – C: coupled drying and carbonation conditions

Fig. 8 shows the evolution of saturation degree profiles at different times in the conditions D for a CEM I cement paste [Fig. 8a] and for the GGBS cement paste [Fig.8b]. For both binders, the saturation degree decreases when the depth goes to the surface due to drying. For the CEM I cement paste [Fig. 8a], the surface seems to be close to equilibrium with the atmosphere from t_0+28 days. The depth affected by the drying at t_0+7 days is 3 cm and 5 cm from t_0+28 days. For the slag cement paste [Fig. 8b], the surface seems to be close to equilibrium with the atmosphere from t_0+7 days. The depth impacted by the drying at t_0+7 days is 4 cm and 6 cm from t_0+28 days. After 56 days profiles for both pastes are very similar. The difference of saturation evolution can be explained by an initial faster drying (t < 7 days) in the slag cement paste due to a higher porosity as shown by the MIP results and the mass loss kinetics.

For the PCM [Figure 9a], the profiles obtained in both conditions C and D at 56 days and 118 days are similar. Therefore, profiles do not seem to be affected by the carbonation. This can be explained by the low carbonation depth (2 mm at 118 days). For the P6S [Fig. 9b], the saturation degree changes at the surface between both conditions. At the surface in the condition D, the saturation is 48 % and in the condition C, is 21 %. Therefore, carbonation seems impact the sorption isotherm. This can be due to a modification of the pore structure of gel as observe in the Figure 7b.

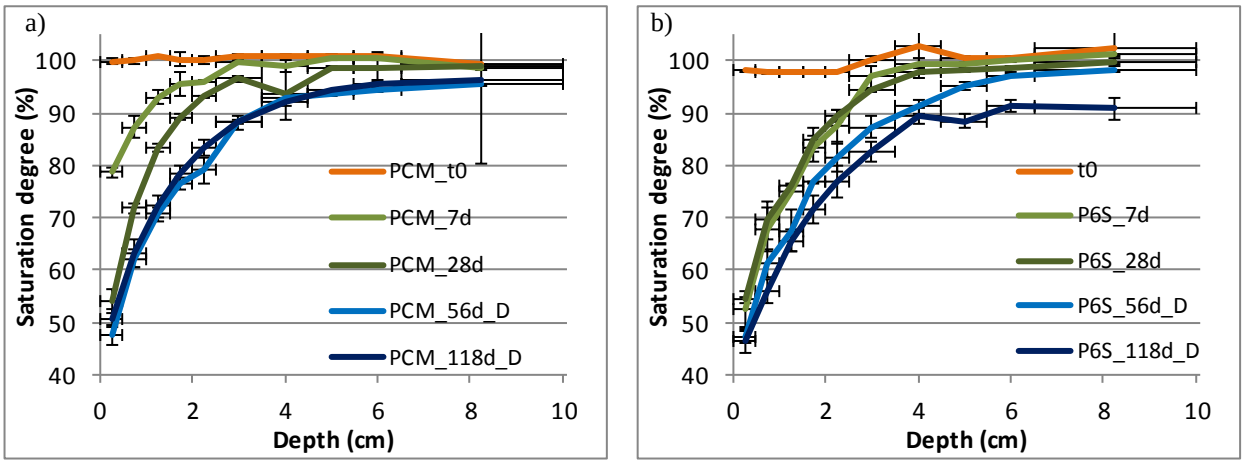

Figure 8: Evolution of saturation degree profiles with the time for PCM (a) and for P6S (b)

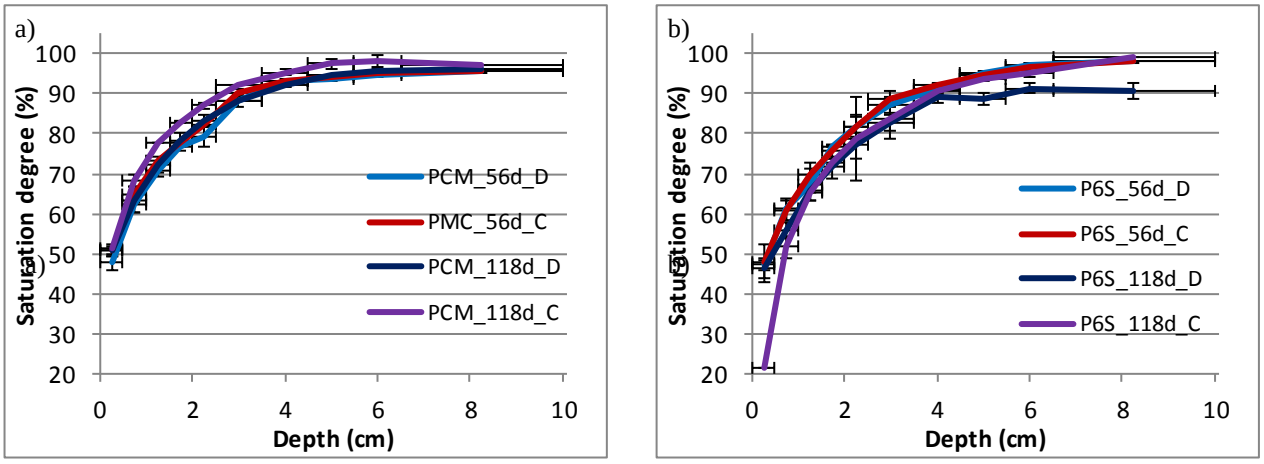

Figure 9: Comparison of saturation degree profiles in D and C conditions for PCM (a) and for P6S (b)

Shrinkage

Evolutions of total shrinkage versus the time are shown in Fig. 10a. For both binders, at the beginning, the specimens swell. This can be due to thermal expansion and hydraulic pressure. In the drying condition, the shrinkage for the M6S (-570 µm/m) is about 3 time higher than MCM (-200 µm/m) as observed by Güneyisi [14]. This can be due to a finer pore structure of M6S which lead to a higher capillary pressure as shown by MIP results [Fig. 6 a & b]. For both binders, total shrinkage in the drying and carbonation conditions is higher than one obtained in the drying condition. Therefore, the carbonation increases the shrinkage value as mentioned by Kamimura [15].

On the other hand, evolutions of carbonation shrinkage versus the time are shown in Fig. 10b. This carbonation shrinkage is 1.2 time higher for the M6S (- 950 µm/m) than the MCM (- 780 µm/m). This can be explained by the carbonation of C-S-H as observed by Chen [13] who explain that the main mechanism of shrinkage is the decalcification of C-S-H. For a C/S below 1.2, this shrinkage becomes non negligible. Moreover, when slag is used, the initial C/S and the carbonation resistance are lower than CEM I. Therefore the C/S is rapidly reduced faster below 1.2 and the carbonation shrinkage is higher. When carbonation shrinkage to drying shrinkage ratio is calculated, the obtained value for MCM is 3.9 and for M6S is 1.67. Therefore, these results confirm the considerable part of carbonation shrinkage in the total one for both binders.

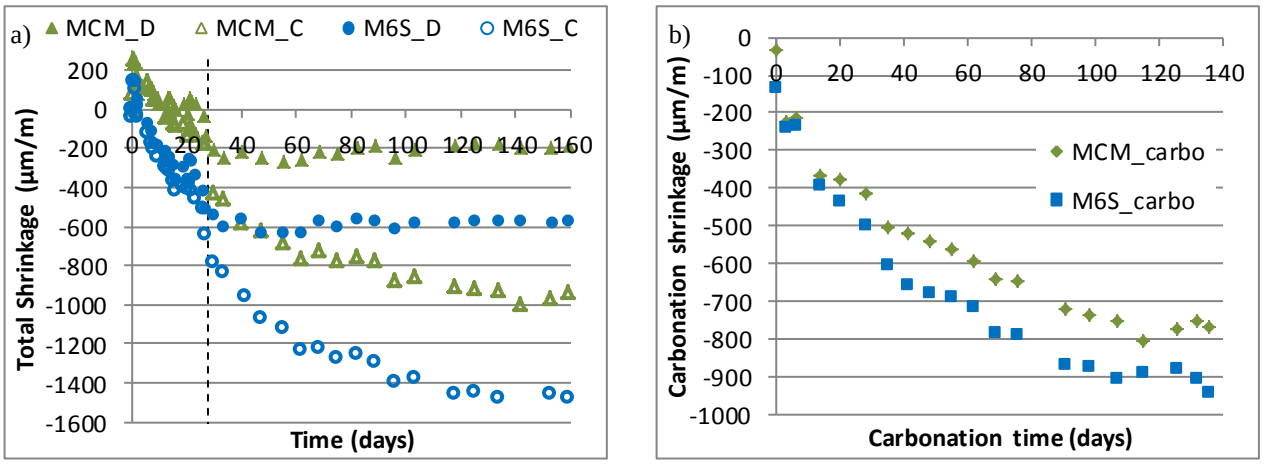

Figure 10: Evolution of total shrinkage (a) and carbonation shrinkage (b) versus time for MCM and M6S

D: T=20°C, RH=65%, [CO_2]=0% – C: T=20°C,RH=65%, [CO_2]=10%

Conclusion

- The carbonation resistance of P6S is lower than PCM as shown by the carbonation kinetics and the $CaCO_3$ content. The carbonation depth at 188 days in the condition C is 5.4 mm for the GGBS cement paste compared to 2.3 mm for the CEM I cement paste. Likewise, the $CaCO_3$ content is higher for the CEM I +60% GGBSSCMs paste (55% after 90 days of carbonation) in comparison with CEM I paste (34% at 90 days of carbonation). The same applies to the C-S-H and aluminates where the carbonation remains higher for slag cement paste ($\Delta n_{C\bar{C}} / \Delta n_{CH}$ =6) than CEM I cement paste ($\Delta n_{C\bar{C}} / \Delta n_{CH}$ =1.8). In the CEM I cement paste, the porosity is fill by the $CaCO_3$ which lead to decrease the main pore diameter. In the GGBS cement paste case, the carbonation of C-S-H leads to a coarser porosity of gel. The pore diameter at 6 nm increases until 20 nm after carbonation. This change of pore structure of gel seems lead to decreases the saturation at the surface (S = 48 % in condition D and S = 21% in the condition C).
- The drying shrinkage is higher for the CEM I + 60% GGBS mortar (ε_D=-570 µm/m) than CEM I (ε_D=-200µm/m).This can be explained by the finer porosity of GGBS mortar which leads to a higher capillary pressure. The same applies to the carbonation shrinkage which is higher for the CEM I +60% GGBS mortar (ε_c=-950 µm/m) than CEM I mortar (ε_c=-780µm/m) after 90 days at [CO_2]=10%.

Acknowledgements

The authors would like to thank Nanocem (nanocem.org) for the funding of this research and M. SAILLIO for TGA/DTA measurements.

References

[1] I. Fernandez, J. M. Bairán, et A. R. Marí, Corrosion effects on the mechanical properties of reinforcing steel bars. Fatigue and σ–ε behavior, Constr. Build. Mater. 101 (2015) 772−783.

[2] S. Goñi et C. Andrade, Synthetic concrete pore solution chemistry and rebar corrosion rate in the presence of chlorides, Cem. Concr. Res. 20 (1990) 525−539.

[3] C. Alonso, C. Andrade, M. Castellote, et P. Castro, Chloride threshold values to depassivate reinforcing bars embedded in a standardized OPC mortar, Cem. Concr. Res. 30 (2000) 1047−1055.

[4] L. J. Parrott, Some effects of cement and curing upon carbonation and reinforcement corrosion in concrete, Mater. Struct. 29 (1996) 164−173.

[5] M. Thiery, Modélisation de la carbonatation atmosphérique des matériaux cimentaires , PhD thesis (2005).
[6] P. H. R. Borges, J. O. Costa, N. B. Milestone, C. J. Lynsdale, et R. E. Streatfield, Carbonation of CH and C–S–H in composite cement pastes containing high amounts of BFS, Cem. Concr. Res. 40 (2010) 284−292.
[7] E. Gruyaert, P. Van den Heede, et N. De Belie, Carbonation of slag concrete: Effect of the cement replacement level and curing on the carbonation coefficient – Effect of carbonation on the pore structure, Cem. Concr. Compos. 35 (2013) 39−48.
[8] A. Morandeau, M. Thiéry, et P. Dangla, Impact of accelerated carbonation on OPC cement paste blended with fly ash, Cem. Concr. Res. 67 (2015) 226−236.
[9] E. G. Swenson et P. J. Sereda, Mechanism of the carbonatation shrinkage of lime and hydrated cement, J. Appl. Chem. 18 (1968) 111−117.
[10] Y. F. Houst, Carbonation shrinkage of hydrated cement paste, in Proc. 4th CANMET/ACI International Conference on Durability of Concrete, (1997) 481-491.
[11] B. Persson, Eight-year exploration of shrinkage in high-performance concrete, Cem. Concr. Res. 32 (2002) 1229-1237.
[12] F. Matsushita, Y. Aono, et S. Shibata, Calcium silicate structure and carbonation shrinkage of a tobermorite-based material, Cem. Concr. Res. 34 (2004) 1251-1257.
[13] J. J. Chen, J. J. Thomas, et H. M. Jennings, Decalcification shrinkage of cement paste, Cem. Concr. Res. 36 (2006) 801-809.
[14] E. Güneyisi, M. Gesoğlu, et E. Özbay, Strength and drying shrinkage properties of self-compacting concretes incorporating multi-system blended mineral admixtures, Constr. Build. Mater. 24 (2010) 1878‑ 1887.
[15] K. Kamimura, P. J. Sereda, et E. G. Swenson, Changes in weight and dimensions in the drying and carbonation of Portland cement mortars, Mag. Concr. Res. 17 (1965) 5−14.